Published in final edited form as:

*Ocul Surf*. 2018 January ; 16(1): 101–111. doi:10.1016/j.jtos.2017.09.004.

# In Vivo Confocal Microscopy Detects Bilateral Changes of Corneal Immune Cells and Nerves in Unilateral Herpes Zoster Ophthalmicus

**Bernardo M. Cavalcanti, MD**[1,2], **Andrea Cruzat, MD**[1], **Afsun Sahin, MD**[1,3,4], **Deborah Pavan-Langston, MD**[1], **Eric Samayoa, MD**[1], and **Pedram Hamrah, MD.**[1,4,5]

[1]Ocular Surface Imaging Center and Cornea & Refractive Surgery Service, Massachusetts Eye & Ear Infirmary, Department of Ophthalmology, Harvard Medical School, 243 Charles Street, Boston, MA 02114, USA

[2]Post-Graduatate Program, Surgery Department, Pernambuco Federal University (UFPE), Recife, PE, Brazil

[3]Koc University Medical School, Research Center for Translational Medicine, Istanbul, Turkey

[4]Boston Image Reading Center, Boston, MA

[5]Cornea Service, New England Eye Center, Department of Ophthalmology, Tufts Medical Center, Tufts University School of Medicine, Boston, MA

## Abstract

**Purpose—**To analyze bilateral corneal immune cell and nerve alterations in patients with unilateral herpes zoster ophthalmicus (HZO) by laser in vivo confocal microscopy (IVCM) and their correlation with corneal sensation and clinical findings.

**Materials and Methods—**This is a prospective, cross-sectional, controlled single-center study. Twenty-four eyes of 24 HZO patients and their contralateral clinically unaffected eyes and normal controls (n=24) were included. Laser IVCM (Heidelberg Retina Tomograph/Rostock Cornea Module), corneal esthesiometry (Cochet-Bonnet) were performed. Changes in corneal dendritiform cell (DC) density and morphology, number and length of subbasal nerve fibers and their correlation to corneal sensation, pain, lesion location, disease duration, and number of episodes were analyzed.

**Results—**HZO affected and contralateral eyes showed a significant increase in DC influx of the central cornea as compared to controls (147.4±33.9, 120.1±21.2, and 23.0±3.6 cells/mm2; $p<0.0001$). In HZO eyes DCs were larger in area (319.4±59.8 $\mu m^2$; $p<0.001$) and number of dendrites (3.5±0.4 n/cell; $p=0.01$) as compared to controls (52.2±11.7, and 2.3±0.5). DC density

Corresponding author: Pedram Hamrah, M.D., Department of Ophthalmology, Tufts Medical Center, Tufts University School of Medicine, Boston, MA, U.S.A., Tel: +1-617-636-5321; Fax: +1-617-636-1466; pedram.hamrah@tufts.edu; p_hamrah@yahoo.com.

The authors have no commercial or proprietary interest in any concept or product discussed in this article.

and size showed moderate negative correlation with total nerve length (R=−0.43 and R=−0.57, respectively; all p<0.001). A higher frequency of nerve beading and activated DCs close to nerve fibers were detected specifically in pain patients.

**Conclusions—**Chronic unilateral HZO causes significant bilateral increase in corneal DC density and decrease of the corneal subbasal nerves as compared to controls. Negative correlation was observed for DC density and size to nerve parameters, suggesting interplay between the immune and nervous systems. Patients with chronic pain also showed increased nerve beading and activated DCs.

### Keywords

Confocal microscopy; Corneal nerves; Corneal sensation; Dendritic cells; Herpes zoster ophthalmicus; Neurotrophic keratopathy

## 1. INTRODUCTION

Herpes zoster (HZ), commonly called shingles, results from reactivation of varicella-zoster virus (VZV) infection. The virus remains dormant in the dorsal root or other sensory ganglia after the primary varicella (chickenpox) infection[1–3]. The trigeminal ganglion is the most frequent site of latency (65–90%) for VZV[4]. In the United States, 1 million new cases are reported per year[5]. Typically, the incidence of HZ increases with age, as well as with diseases and drugs, which can lead to immunosuppression. Herpes zoster ophthalmicus (HZO) is defined as HZ involvement of the ophthalmic division of the trigeminal nerve. HZO is the second most common type of HZ. It accounts for 20% of all cases and approximately 50% of patients will have ocular involvement [6–10]. Herpes zoster can affect virtually every ocular tissue, resulting in conjunctivitis, scleritis, keratitis, uveitis, keratouveitis, and endotheliitis. Nearly two-thirds of patients with HZO demonstrate a keratitis that often is associated with loss of corneal sensation. Corneal complications can occur due to inflammatory and immune reaction to the virus, vasculopathy, and neuropathy, and may commonly present with neurotrophic keratitis. Neurotrophic keratitis then results in dry eye disease, persistent corneal epithelial defects, inflammation, corneal melting, and potentially perforation, possibly leading to significant vision loss or legal blindness.

Dendritic cells of the cornea play a major role in the immune defense against the external environment [11, 12]. These professional antigen presenting cells are essential regulators of both the innate and adaptive immune systems. Dendritic cells are widely distributed on the ocular surface and are specialized to capture, process, and present antigens to other immune cells. Interestingly, in vitro and skin biopsy studies have shown the importance of dendritic cells as a carrier of VZV to draining lymph nodes and in the transmission of the virus to T lymphocytes [13–16]. However, the role of dendritic cells in the cornea of HZO patients has not been previously explored in vivo.

Corneal nerve damage is likely to occur after viral infections (herpes simplex and herpes zoster) [17–19]. Nearly two-thirds of patients with HZO will develop loss of corneal sensation due to nerve damage, necrotic ganglionitis, or damage to the mesencephalic nucleus in the brainstem [20]. Corneal nerve fibers exert important trophic influences on the

ocular surface, and a large number of nerves contain substance P (SP) and/or calcitonin gene-related peptide (CGRP). Cornea sensory nerves interact with the epithelium through soluble mediators, such as SP, and are essential to the ocular surface homeostasis and function [21, 22]. Recent reviews have shown the correlation between corneal nerve alterations and sensation [23, 24]. Thus, the loss of sensation as a result of nerve damage can lead to neurotrophic keratopathy (NTK), which represents one of the most challenging ocular diseases. The prognosis of NTK depends mainly on the level of hypo- or an-esthesia and its consequences, which can result in other conditions, such as dry eye disease, exposure keratopathy, neurotrophic ulcers, and limbal stem cell deficiency.

In vivo confocal microscopy (IVCM) is a novel tool that allows for quasi-histological in vivo optical sections of the cornea, increasing the understanding of anatomy and pathology in diseased eyes. It allows physicians to visualize the nerve plexus and cellular changes that are not visible by conventional slit-lamp bio-microscopy. In particular, laser IVCM enables the assessment of dendritiform immune cells (DCs) and corneal nerves at a high resolution in normal subjects and in patients after ocular surgery (refractive and keratoplasty), dry eye disease, immune-mediated inflammatory diseases such as herpetic keratitis and infectious keratitis [23, 25–31].

Interestingly, our group has recently shown that clinically apparent unilateral diseases such as herpes simplex keratitis and HZO demonstrate contralateral loss of the corneal nerves plexus compared to controls [32–34]. Moreover, a recent study by Cruzat et al. [35] suggested a connection between the immune system and nervous system in patients with acute bacterial, fungal and Acanthamoeba keratitis using laser IVCM. Given that there is an inflammatory response during the course of corneal herpes infections, it is important to elucidate this interaction by means of DCs and subbasal nerve plexus [36]. However, there is very limited data about the immune cell/nerve interactions in human corneas during the course of herpes infections. Thus, we hypothesize that immune cell alterations correlate to subbasal nerve changes in HZO patients. To begin testing this hypothesis, we used IVCM to detect bilateral immune cell alterations and the extent of subbasal nerve damage in patients with unilateral HZO and correlated the IVCM findings with clinical findings.

## 2. METHODS

### 2.1. Patients

This study was performed in a prospective, cross-sectional, controlled, single-blinded fashion. Twenty-four patients with diagnosis of unilateral HZO with ocular involvement were recruited between 2010 and 2012 from the Cornea Service of the Massachusetts Eye and Ear Infirmary, Boston, MA. All affected eyes had chronic disease defined by the absence of epithelial keratitis or clinical active stromal keratitis after the initial episode. Both eyes, affected and contralateral clinically unaffected, were included as separate groups. Twenty-four eyes of 24 normal volunteers comprised the control group. Only one eye of each subject was randomly chosen. Subjects with a history of infectious keratitis, ocular inflammatory disease, ocular trauma, ocular surgery, contact lens use, diabetes, systemic neuropathies or immunosuppression were excluded. The study was Health Insurance Portability and Accountability Act-compliant and was approved by the Institutional Review

Board/Ethics Committee. The tenets of the Declaration of Helsinki were followed. Prior to study, written informed consent was obtained from all study subjects.

### 2.2. Clinical examination and Corneal Sensation

All patients underwent examination by slit-lamp biomicroscopy and central corneal sensation (DP-L, PH) was measured with a contact Cochet-Bonnet esthesiometer (Luneau Ophthalmologie, Chartres, France). Clinical information, specifically time from disease onset, number of inflammatory episodes, and pain grade based on visual analogue scale [37] were obtained. Inflammatory episodes were considered as both primary and secondary immune keratitis. Pain was characterized by the presence of pain and controlled pain was characterized in patients with concurrent use of pain medications. The Cochet-Bonnet esthesiometer, which stimulates the corneal nerves mechanically, has a retractable monofilament nylon thread (6 cm length, 0.12 mm diameter). If a positive response is not obtained, it shortens in steps of 1.0 cm. If a positive response is obtained, the thread is progressed by 0.5 cm until a positive response is not obtained. This test was repeated twice, both times at the center of the cornea. The longest filament length resulting in a positive response was recorded. The affected eye group was subdivided into three subgroups according to location of corneal scar into clear (absence of scar), central, and peripheral.

### 2.3. Laser In Vivo Confocal Microscopy

Laser scanning in vivo confocal microscopy (Heidelberg Retina Tomograph 3 with Rostock Cornea Module, Heidelberg Engineering GmbH, Heidelberg, Germany) images of central corneas were obtained in all subjects. The HRT3/RCM is a contact confocal microscope constructed to examine the ocular surface in vivo. It operates with a 63x objective immersion lens (Olympus, Tokyo, Japan), allowing a scanning area of 400 × 400μm with a magnification up to 800 times and a resolution of approximately 1μm.

We imaged the patients with a previously described technique [35]. Briefly, the bottom of a single use sterile polymethylmethacrylate cap (Tomo-Cap; Heidelberg Engineering GmbH, Heidelberg, Germany) was filled with an appropriate amount hydroxypropyl methylcellulose 2.5% (GenTeal gel, Novartis Ophthalmics) and was mounted in front of the Rostock Cornea Module optics for each examination. Each patient received one drop of 0.5% proparacaine hydrochloride (Alcaine, Alcon, Ft. Worth, TX) and one drop of hydroxypropyl methylcellulose 2.5% (GenTeal gel, Novartis Ophthalmics) in both eyes, respectively. Before examination, in order to improve optical coupling, one drop of hydroxypropyl methylcellulose 2.5% was also placed on the outside tip of the Tomo-Cap. The cornea module was manually advanced until the gel contacted the central surface of the cornea.

A particular focus on the subbasal nerve plexus and epithelial DCs was adapted. A total of 6 sequence scans were obtained from the center of each cornea with and this yielded 300–400 images of the subbasal layer per subject. Digital images were stored on a network computer at 3 frames/per second.

### 2.4. Image Analysis

At least 50 good quality images from the cornea, which were the best focused and complete in the same layer images, with good contrast, and without motion or folds, were chosen by an experienced masked observer. Of these, the same observer selected a minimum of three representative images of the subbasal nerve plexus and epithelial dendritiform immune cells (DCs) for analysis.

Chosen confocal images were analyzed for central corneal DC density and the density of subbasal nerve plexus by two masked observers as previously described [35]. IVCM images at 50–70 μm depth at the level of basal epithelial layers, basal lamina, or subbasal nerve plexus were chosen for analysis of DCs. DCs were morphologically identified as bright individual dendritiform structures with cell bodies that allowed us to differentiate these structures from the corneal nerves. The following parameters were determined for each image, as explained below: DC density, DC size (the area covered by the body of the cell), number of dendrites per DC, and DC field (area bounded within the span of the dendrites) [38]. DCs were counted using software (Cell Count, Heidelberg Engineering GmbH) in the manual mode. The data were expressed as density (cells/$mm^2$) ± SD [35].

DC size and number of dendrites per DC were measured using ImageJ, a free image analysis software distributed by the National Institutes of Health (http://rsb.info.nih.gov/ij/http://rsb.info.nih.gov/ij/). Briefly, cell density was manually counted and data were expressed as cells/$mm^2$ ± standard error of the mean (SEM). Cell count tool in the manual mode was used to analyze the DC density per image. All complete DCs present in each image, as well as partial cells on the top and right borders of each frame were counted and included in the calculation of the average density of DCs. For each calculation, the mean of three images was used. For the morphologic analysis, the 10 most representative cells in three images for each eye were chosen. DC size reflects the actual hyperreflective DC structure and DC field represents the area surrounding the DC by connecting all dendrites. DC size and field were reported as $\mu m^2$ ± SEM. Threshold function was used to measure the size of the DC. The number of dendrites per cell was calculated manually. The representative of the cell span and the length of the dendritic processes were considered as DC field. It was calculated by measuring the area covered by a polygon joining the dendrite tips around each cell.

NeuronJ, which is a semi-automated tracing program (a plugin for ImageJ), was used to analyze corneal nerves. (http://www.imagescience.org/meijering/software/neuronj/) [39]. The whole frame was analyzed for the presence of main trunks, branches, and total nerves. Total number of main nerve trunks was counted in each image after analyzing anteriorly and posteriorly in order to confirm that main nerve trunks did not branch from other nerves. Total number of nerve branches was calculated by the sum of nerve branching. The number of total nerves measured was defined as the number of all nerves, including main nerve trunks and branches in one image. Nerve length was assessed by measuring the length of the nerve fibers in micrometers per mm2 ± SEM. Two masked observers evaluated all the images and the averaged values were used for the analysis. If there was more than 10% difference between the two observers, a third observer evaluated the images as well and the average of these three values was used for the analysis.

### 2.5. Statistical Analysis

The normal distribution of the data was first confirmed with the Shapiro-Wilk test. Student's T-test and X-squared were used to assess the differences of age and gender between HZO and control groups. Statistical analysis was carried out through an analysis of variance (ANOVA) with Bonferroni correction to compare all corneal sensation and IVCM parameters. A Pearson R coefficient analysis was used to address the correlation between all parameters. Further, Fischer's exact test was used to compare the subbasal nerves changes in patients with pain versus no pain. Finally, a receiver operating characteristic (ROC)-curve model was applied to assess the specificity and sensitivity of the nerves parameters and corneal sensation. All quantitative variables were expressed by the mean and SEM. Differences were considered statistically significant for p less than 0.05. Analyses were performed with SPSS software version 18.0 (Statistical Package for Social Sciences, Chicago).

## 3. RESULTS

Twenty-four eyes of 24 HZO patients with unilateral ocular involvement, as well as their respective contralateral clinically unaffected eyes, were included. HZO patients were compared to 24 normal eyes of 24 age- and gender-matched volunteers. The mean age and male/female ratio were 60.1 ± 3.0 years and 11/13 for the HZO group, and 55.6 ± 1.9 years and 9/15 for controls (p=0.2 for age and p=0.5 for gender). Both groups were homogenous and no statistical difference was found for age and sex variables. A summary of demographics is provided in Table 1.

### 3.1. Dendritiform Cell Density

Dendritiform immune cells were located in the subbasal layer. Quantitative analysis of the DC density and morphology for HZO patients and the normal control group is shown in Table 2 and Figure 1.

Eyes affected with HZO showed a significant increase in DC density compared to controls (141.2 ± 33.7 vs. 23.0 ± 3.6 cells/mm2; p<0.001 [Figure 2]). In addition, the contralateral clinically unaffected eyes had an increase in DC density similar to the affected eyes, with DC density being significantly higher (120.1 ± 21.2; p<0.001) in comparison to controls. Interestingly, DCs in HZO eyes were larger with increased number of dendrites. Particularly, DC size (319.4 ± 59.8 μm2), DC field (787.8 ± 164.9 μm2) and number of dendrites (3.5 ± 0.4 dendrites per cell) were increased in the affected eye in comparison to controls (57.2 ± 11.7, 182.4± 37.2, and 2.3 ± 0.5; p<0.001 [Figure 2]). Further, when compared to controls, contralateral eyes showed increased DC size (161.9 ± 33.1 vs. 57.2 ± 11.7; 35.3% increase), DC field (312.0 ± 63.7 vs. 182.4 ± 37.2; 58.4% increase), and number of dendrites (3.1 ± 0.6 vs. 2.3 ± 0.5; 74.1% increase), but no statistical significance was found in comparison to controls (p=0.291, p=0.977 and p=0.277; respectively [Figure 2]).

After subdividing the HZO patients by location of corneal involvement into clear cornea, central or peripheral scar, no statistical difference was found between groups for DC changes in the central cornea (p=0.8). However, at the time of the visit when imaging was performed,

one fourth of the patients (6/24) had clinical inflammation characterized by conjunctival redness, increased blurriness and discomfort, or by the physician's recommendation to increase steroids drops. DC density was 60% higher in this subset of patients (170.1 ± 73.5 cells/mm2) as compared to patients with quiet eyes (100.6 ± 21.5).

### 3.2. Subbasal Nerve Changes

Quantitative analysis of nerve parameters for patients with HZO and the normal control group is listed in Table 2. Eyes affected with HZO and contralateral clinically unaffected eyes showed a significant reduction in the subbasal nerve plexus parameters as compared to controls (Fig. 3 and Fig. 4, including: total nerve length (9,052.6 ± 1,151.4, 14,959.8 ± 903.2, and 22,851.4 ± 661.4 μm/mm2 respectively; all $p<0.001$), total number of nerves (5.8 ± 0.9, 11.9 ± 1.2, and 26.6 ± 1.2 n/frame; all $p<0.001$), number of main nerve trunks (2.4 ± 0.3, 3.8 ± 0.3, and 4.4 ± 0.2; all $p<0.001$) and the number of branches (3.4 ± 0.7, 8.2 ± 1.1, and 22.2 ± 1.2; all $p<0.001$). Bonferroni multiple comparison tests did not show statistical difference between the contralateral eye and controls for the number of main trunks.

In particular, when subgroups were divided according to the presence and location (central vs. periphery) of corneal scars, the total nerve length (12,991.3 ± 1,044.9, 7,798.4 ± 1,772.4, 9,411.8 ± 1,843.0, $p=0.368$), total number of nerves (8.1 ± 1.3, 5.5 ± 1.5, and 5.6 ± 1.3 n/frame; $p=0.648$), number of main nerve trunks (3.4 ± 0.5, 2.0 ± 0.4, and 2.6 ± 0.5; $p=0.267$) and the number of branches (4.7 ± 1.2, 3.4 ± 1.2, and 3.0 ± 0.8; $p=0.777$) were not statistically different, although patient with no scars demonstrated a higher nerve density.

### 3.3. Correlation and Regression Analysis

No statistical difference was found for the subbasal nerve measurements and DC parameters when comparing the affected eyes of HZO patients with or without pain (Table 3). Interestingly, a higher frequency of beading (92.8% vs 60.0%; $p=0.024$), cluster of cell nuclei (64% vs 10%; $p=0.006$), and activated DCs close to nerve fibers (<20μm from fibers) (85.7% vs 50.0%; $p=0.035$) was detected in pain patients as shown in Fig. 5. All HZO patients had similar frequency of microneuromas (41.6%) at the subbasal nerve plexus.

Pearson's correlation coefficient was used in order to correlate the DC density with all nerve parameters. The increase of DC density had statistically significant negative correlation to total nerve length, total number of nerves, and number of nerve branches ($R=-0.43$, $R=-0.57$, $R=-0.63$; respectively) for all parameters ($p<0.001$). Similar correlations were found for DC size ($R=-0.57$, $p<0.001$), DC field ($R=-0.53$, $p<0.001$), and number of dendrites shown ($R=-0.41$, $p<0.001$) to total nerve length (Figs. 6A, B).

In addition, IVCM nerve parameters were correlated to loss of their function, as measured by the corneal sensation. We observed a significant correlation between the diminishment of the subbasal nerve plexus and the reduction in corneal sensation. Corneal sensation was significantly correlated to total nerve length ($R=0.63$, $p<0.001$ [Fig. 6C]), total number of nerves ($R=0.55$, $p<0.001$), main nerve trunks ($R=0.56$, $p<0.001$), and number of branches ($R=0.51$, $p<0.001$).

A ROC-curve model was performed to calculate the approximate corneal nerve length needed for normal sensation. The estimated area under the curve was 0.940 ± 0.032. We found that abnormal sensation (≤5.5cm) is noted with a total nerve length of 16,067.4 μm/mm2 with 95% of sensitivity and 87% of specificity (Fig. 6D).

A multiple regression model was applied to evaluate the correlation between all IVCM parameters with age, number of episodes, and disease duration. No statistical difference was found for any variable (all $p>0.05$).

## 4. DISCUSSION

Our data presented herein demonstrate the increase of corneal DCs and the diminishment of subbasal nerves in both eyes of patients with clinically unilateral HZO. Previous data using laser IVCM in patients with HZO consist of only a single case report that showed diminishment of nerves only in the affected eye [40]. Recently, our group reported bilateral subbasal nerve changes using a slit-scanning confocal microscopy (SSCM) in 27 cases with unilateral HZO [32]. However, the axial resolution of SSCM (25μm) is significantly lower in comparison to laser scanning technology (1μm) [31]. Thus, the laser IVCM provides not only further detail of subbasal nerves, but allows for assessment of corneal immune cells in HZO, which has not been studied to date.

Immunohistochemical studies have shown the presence of DCs within the normal corneal tissue in animal and human studies [12, 41, 42]. Our group has also extensively studied DCs in human corneas by means of IVCM [12, 42–46]. DCs act as sentinels, monitoring the adjacent tissue for foreign stimuli and undergo activation due to various stimuli [12, 46]. Dendritic cells have been shown to be critical for the initiation of adaptive immune responses and for maintenance of peripheral tolerance [11]. Previous IVCM studies have shown the presence of epithelial DCs in the central cornea healthy volunteers [28, 47, 48]. Mature phenotyes of DCs are characterized by large cells with long processes and are observed in both eyes of our HZO patients [47]. In addition, we have recently demonstrated bilateral increase DC density and size in patients with unilateral acute bacterial fungal, and Acanthamoeba keratitis [35, 49].

In the current study, we detected a significant increase in DC density in both affected and clinically unaffected contralateral eyes in patients with chronic unilateral HZO as compared to controls. However, in contrast to our previous studies, the increase in DC density is present in patients with a chronic condition, as the mean follow-up period is 57 months, suggesting that inflammation or immune activation persists in HZO patients long after the active stage of the disease. We have shown that the increase in DC density significantly correlates to increased levels of pro-inflammatory tear cytokine levels [50], which are elevated bilaterally in patients with unilateral bacterial keratitis, suggesting chronic inflammation in our HZO cohort. However, specific mechanisms have to be substantiated by comprehensive studies in animals and humans to determine the sequence of events that take place after HZO with regard to DC and subbasal nerve alterations.

The connection between the immune and nervous systems has been the focus of recent studies [51–54]. It has been postulated that the neuro-immune cross-talk occurs through the interaction of cytokines and interleukins produced by leukocytes to receptors expressed on nerves and cells of the neuroendocrine system. This interplay constitutes an important feedback loop that optimizes the inflammatory response to pathogens[55]. Namavari et al. [56] reported the link between Sema7a, a glycosylphosphatidylinositol (GPI)-anchored membrane-associated semaphorin, and the inflammatory cell influx into the cornea. Cruzat et al. [35] have previously demonstrated an increase in corneal DCs with decreased subbasal nerve plexus in acute infectious keratitis in humans. In the current study, the increase of corneal DC density and DC size correlated negatively with the diminishment of the subbasal nerves as well, suggesting that this interaction may not be disease-specific.

Corneal sensation is a subjective method of assessing corneal nerve function [57]. The cornea is the most densely innervated tissue in the human body, supplied by the terminal branches of the ophthalmic division of the trigeminal nerve as ciliary nerves [58]. IVCM has been used to characterize the subbasal nerve plexus in normal and diseased eyes by the presence of hyperreflective fibers [23, 59]. Previous IVCM studies have shown a significant correlation between nerve parameters and corneal sensation in herpes simplex, in other types of acute infectious keratitis, and in patients with bullous keratopathy [25, 33, 35]. However, herein we demonstrated a sensitivity of 95% and a specificity of 87% through a ROC curve, and a cut-offvalue of 16,067.4 μm/mm2 for total nerve length for diminished corneal sensation (corneal sensation ≤ 5.5cm). This methodology demonstrates the high precision of laser IVCM in the detection of corneal subbasal nerves.

Pain is one of the most common complications in patients with HZO [8]. In this study, 14 out of 24 patients presented with pain at the time of the visit. A previous report by Oaklander et al. showed reduction of nerve fibers in skin biopsies of patients with HZO and post-herpetic neuralgia as compared to patients without pain [60]. In our series, however, we showed no statistical difference for subbasal corneal nerves when comparing patients with and without pain. A possible explanation for the discrepancy is the much higher (more than 300-fold) density of nerve fibers in the cornea in comparison to the skin [61]. However, laser IVCM detects a higher frequency of morphological subbasal changes in patients with pain, who particularly presented with nerve beading, clusters of cell nuclei, and increase in activated DCs close to nerve fibers. Reports have shown that cytokines released from immune cells can directly impact neuronal function, resulting in spontaneous (ectopic) activity and pain [62]. Particularly, pro-inflammatory cytokines, including interleukin (IL)-1, IL-6, and tumor necrosis factor (TNF)-a can directly modulate neuronal activity and evoke spontaneous action potential discharges. Animal models have demonstrated attenuation of neuropathic pain through blockade of IL-1 or IL-6 [63, 64]. Further, Wolf et al.[63] demonstrated minimal ectopic activation of axon in mice with target deletion of IL-1 receptor. Additionally, subcutaneous injection of TNF-α in rats, sensitizes C nociceptors leading to lower thresholds in 66.7% of fibers and evoking ongoing activity in 14% of nociceptors [65]. Future studies assessing corneal IVCM and skin biopsies in the same patients, as well as the assessment of the peripheral cornea by IVCM, may shed additional light.

The contralateral DC changes in the clinically unaffected eyes in unilateral HZO patients were surprising and novel. In a histopathological study of 21 unilateral shingles cases, gross hemorrhagic necrosis and inflammatory infiltrates were reported in skin tissues of the affected site, but never in the contralateral side [66]. On the other hand, bilateral changes in unilateral HZ have recently been reported in epidermal biopsies [67]. Oaklander and co-workers performed skin biopsies after unilateral shingles and analyzed the density of epidermal and dermal neurites [67]. They found that unilateral postherpetic neuralgia patients also showed contralateral loss of epidermal neurites [67]. Our results are consistent with this study that showed milder contralateral changes [67]. A neurogenic interaction has been proposed as a result of contralateral diminishment of corneal nerves, and the neuro-immune cross-talk may explain the bilateral sympathetic immune changes observed [67]. The evidence for contralateral effects of clinically unilateral focal nerve injuries has been increasing in both the ocular and non-ocular diseases [68]. The observed contralateral nerve loss is likely not due to viral spread, as unilateral axotomy of the ciliary ophthalmic branches of V1 in mice results in similar contralesional changes by day 1 after surgery [69]. Moreover, there are small number of fibers that each eye and other tissues innervated by the trigeminal nerve [70] send to the contralateral peripheral Gasserian ganglion [71, 72]. Moreover, it has been shown that some central axons of peripheral trigeminal afferents project to both the contralateral and ipsilateral central trigeminal nuclei [73]. Strikingly, our group recently showed that contralateral corneal denervation causes leukocyte infiltration in the contralateral asymptomatic eyes with acute unilateral bacterial keratitis [49], further supporting the findings of the present study. In a varicella-zoster virus (VZV) keratitis patient, VZV DNA was detected in the tear film of the both affected and contralateral unaffected eyes [74]. There is also evidence from animal studies. After inoculation of live virus in mice, the virus was shown in the contralateral part of the brainstem as well as in the contralateral eye [75]. Taken together, it is plausible that a coordinated bilateral interaction between the nervous system and the immune system can take place during unilateral corneal diseases. A limitation of the present study is that laser IVCM can only categorize immune cells based on morphology. As previously, reported by Guthoff et al. [76], laser IVCM does not allow the clinician to distinguish cell characteristics such as nuclei or granules. Still, typical cell morphology, diameter of the cell body, and location of the cell aids in the interpretation of the confocal data. Recently, Knickelbein et al. [77] defined the phenotype and location of DCs in normal donor human corneas by fluorescence confocal microscopy and flow cytometry. They determined the phenotype and location of tissue-resident APCs. Confocal fluorescence microscopy was also used to examine the response of corneal resident APCs to ex vivo infection with HSV-1. They confirmed that DCs and Langerhans cells reside in the human corneal basal epithelium and anterior stroma and are likely the source of cells seen on IVCM. Nevertheless, a standard approach to image acquisition and analysis is fundamental to the reproducibility of future studies. In addition, the Cochet-Bonnet esthesiometer is less than ideal for its intended purpose as a consequence of its design, limited stimulus intensity range, user-dependency, variation in stimulus delivered, restrictive stimulation of only mechanoreceptors and lack of reproducibly measuring corneal sensation at low thresholds of stimuli [78, 79]. However, other devices, such as the Belmonte esthesiometer, are currently not commercially available.

## 5. CONCLUSION

Laser IVCM is a powerful tool to assess corneal immune and subbasal nerve changes. The current study quantitatively analyzed corneal immune cells, nerve structure and an aspect of nerve function in patients in vivo. These results provide evidence of neuro-immune crosstalk in the cornea, as the data presented reveals a moderate correlation of DC density with subbasal nerve parameters. In addition, a strong correlation with the diminishment of the subbasal plexus and corneal sensation was observed in HZO patients. Thus, quantitative measurements of DCs and subbasal nerve plexus of the cornea may aid in the stratification of patients for therapeutic interventions, allowing a direct evaluation of treatment response and future complications. Further, longitudinal studies are needed to validate these findings and the correlation with other clinical parameters.

## Acknowledgments

Funding/Support: NIH K08-EY020575, NIH R01-EY022695, NIH R21-EY025393 (PH), New England Corneal Transplant Research Fund (PH), Falk Medical Research Foundation (PH), Johnstone Research Fund (DP-L), Stevens Research Fund (DP-L). The funding organizations had no role in the design or conduct of this research.

## References

1. Gnann JW Jr, Whitley RJ. Clinical practice. Herpes zoster. N Engl J Med. 2002; 347:340–6. [PubMed: 12151472]
2. Hope-Simpson RE. The nature of herpes zoster: a long-term study and a new hypothesis. Proc R Soc Med. 1965; 58:9–20. [PubMed: 14267505]
3. Straus SE, Reinhold W, Smith HA, Ruyechan WT, Henderson DK, Blaese RM, et al. Endonuclease analysis of viral DNA from varicella and subsequent zoster infections in the same patient. N Engl J Med. 1984; 311:1362–4. [PubMed: 6092956]
4. Liesegang TJ. Varicella-zoster virus eye disease. Cornea. 1999; 18:511–31. [PubMed: 10487424]
5. Oxman MN, Levin MJ, Johnson GR, Schmader KE, Straus SE, Gelb LD, et al. A vaccine to prevent herpes zoster and postherpetic neuralgia in older adults. N Engl J Med. 2005; 352:2271–84. [PubMed: 15930418]
6. Edgerton AE. Herpes zoster ophthalmicus: Report of cases and a review of the literature. Trans Am Ophthalmol Soc. 1942; 40:390–439. [PubMed: 16693295]
7. Ragozzino MW, Melton LJ 3rd, Kurland LT, Chu CP, Perry HO. Population-based study of herpes zoster and its sequelae. Medicine (Baltimore). 1982; 61:310–6. [PubMed: 6981045]
8. Liesegang TJ. Herpes zoster ophthalmicus natural history, risk factors, clinical presentation, and morbidity. Ophthalmology. 2008; 115:S3–12. [PubMed: 18243930]
9. Harpaz R, Ortega-Sanchez IR, Seward JF. Advisory Committee on Immunization Practices Centers for Disease C, Prevention. Prevention of herpes zoster: recommendations of the Advisory Committee on Immunization Practices (ACIP). MMWR Recomm Rep. 2008; 57:1–30. quiz CE2–4.
10. Schmader KE, Dworkin RH. Natural history and treatment of herpes zoster. J Pain. 2008; 9:S3–9. [PubMed: 18166460]
11. Hamrah P, Dana MR. Corneal antigen-presenting cells. Chem Immunol Allergy. 2007; 92:58–70. [PubMed: 17264483]
12. Hamrah P, Liu Y, Zhang Q, Dana MR. The corneal stroma is endowed with a significant number of resident dendritic cells. Invest Ophthalmol Vis Sci. 2003; 44:581–9. [PubMed: 12556386]
13. Abendroth A, Kinchington PR, Slobedman B. Varicella zoster virus immune evasion strategies. Curr Top Microbiol Immunol. 2010; 342:155–71. [PubMed: 20563710]
14. Abendroth A, Morrow G, Cunningham AL, Slobedman B. Varicella-zoster virus infection of human dendritic cells and transmission to T cells: implications for virus dissemination in the host. J Virol. 2001; 75:6183–92. [PubMed: 11390620]

15. Morrow G, Slobedman B, Cunningham AL, Abendroth A. Varicella-zoster virus productively infects mature dendritic cells and alters their immune function. J Virol. 2003; 77:4950–9. [PubMed: 12663800]
16. Huch JH, Cunningham AL, Arvin AM, Nasr N, Santegoets SJ, Slobedman E, et al. Impact of varicella-zoster virus on dendritic cell subsets in human skin during natural infection. J Virol. 2010; 84:4060–72. [PubMed: 20130046]
17. Bonini S, Lambiase A, Rama P, Caprioglio G, Aloe L. Topical treatment with nerve growth factor for neurotrophic keratitis. Ophthalmology. 2000; 107:1347–51. discussion 51–2. [PubMed: 10889110]
18. Davis EA, Dohlman CH. Neurotrophic keratitis. Int Ophthalmol Clin. 2001; 41:1–11.
19. Bonini S, Rama P, Olzi D, Lambiase A. Neurotrophic keratitis. Eye (Lond). 2003; 17:989–95. [PubMed: 14631406]
20. Pavan-Langston D. Herpes zoster ophthalmicus. Neurology. 1995; 45:S50–1.
21. Muller LJ, Marfurt CF, Kruse F, Tervo TM. Corneal nerves: structure, contents and function. Exp Eye Res. 2003; 76:521–42. [PubMed: 12697417]
22. Garcia-Hirschfeld J, Lopez-Briones LG, Belmonte C. Neurotrophic influences on corneal epithelial cells. Exp Eye Res. 1994; 59:597–605. [PubMed: 9492761]
23. Cruzat A, Pavan-Langston D, Hamrah P. In vivo confocal microscopy of corneal nerves: analysis and clinical correlation. Semin Ophthalmol. 2010; 25:171–7. [PubMed: 21090996]
24. Pritchard N, Edwards K, Shahidi AM, Sampson GP, Russell AW, Malik RA, et al. Corneal markers of diabetic neuropathy. The ocular surface. 2011; 9:17–28. [PubMed: 21338566]
25. Al-Aqaba M, Alomar T, Lowe J, Dua HS. Corneal nerve aberrations in bullous keratopathy. Am J Ophthalmol. 2011; 151:840–9. e1. [PubMed: 21310389]
26. Neira-Zalentein W, Holopainen JM, Tervo TM, Borras F, Acosta MC, Belmonte C, et al. Corneal sensitivity in diabetic patients subjected to retinal laser photocoagulation. Invest Ophthalmol Vis Sci. 2011; 52:6043–9. [PubMed: 21447686]
27. Erie JC, McLaren JW, Hodge DO, Bourne WM. The effect of age on the corneal subbasal nerve plexus. Cornea. 2005; 24:705–9. [PubMed: 16015090]
28. Mastropasqua L, Nubile M, Lanzini M, Carpineto P, Ciancaglini M, Pannellini T, et al. Epithelial dendritic cell distribution in normal and inflamed human cornea: in vivo confocal microscopy study. Am J Ophthalmol. 2006; 142:736–44. [PubMed: 17056357]
29. Patel DV, McGhee CN. Mapping of the normal human corneal sub-basal nerve plexus by in vivo laser scanning confocal microscopy. Invest Ophthalmol Vis Sci. 2005; 46:4485–8. [PubMed: 16303938]
30. Alomar TS, Al-Aqaba M, Gray T, Lowe J, Dua HS. Histological and confocal microscopy changes in chronic corneal edema: implications for endothelial transplantation. Invest Ophthalmol Vis Sci. 2011; 52:8193–207. [PubMed: 21896863]
31. Niederer RL, McGhee CN. Clinical in vivo confocal microscopy of the human cornea in health and disease. Prog Retin Eye Res. 2010; 29:30–58. [PubMed: 19944182]
32. Hamrah P, Cruzat A, Dastjerdi MH, Pruss H, Zheng L, Shahatit BM, et al. Unilateral herpes zoster ophthalmicus results in bilateral corneal nerve alteration: an in vivo confocal microscopy study. Ophthalmology. 2013; 120:40–7. [PubMed: 22999636]
33. Hamrah P, Cruzat A, Dastjerdi MH, Zheng L, Shahatit BM, Bayhan HA, et al. Corneal sensation and subbasal nerve alterations in patients with herpes simplex keratitis: an in vivo confocal microscopy study. Ophthalmology. 2010; 117:1930–6. [PubMed: 20810171]
34. Cruzat A, Hamrah P, Cavalcanti BM, Zheng L, Colby K, Pavan-Langston D. Corneal reinnervation and sensation recovery in patients with herpes zoster ophthalmicus: an in vivo and ex vivo study of corneal nerves. Cornea. 2016; 35:619–25. [PubMed: 26989956]
35. Cruzat A, Witkin D, Baniasadi N, Zheng L, Ciolino JB, Jurkunas UV, et al. Inflammation and the nervous system: the connection in the cornea in patients with infectious keratitis. Invest Ophthalmol Vis Sci. 2011; 52:5136–43. [PubMed: 21460259]
36. Hamrah P, Pavan-Langston D, Dana R. Herpes simplex keratitis and dendritic cells at the crossroads: lessons from the past and a view into the future. Int Ophthalmol Clin. 2009; 49:53–62.

37. Qazi Y, Hurwitz S, Khan S, Jurkunas UV, Dana R, Hamrah P. validity and reliability of a novel ocular pain assessment survey (opas) in quantifying and monitoring corneal and ocular surface pain. Ophthalmology. 2016; 123:1458–68. [PubMed: 27089999]
38. Kheirkhah A, Rahimi Darabad R, Cruzat A, Hajrasouliha AR, Witkin D, Wong N, et al. Corneal epithelial immune dendritic cell alterations in subtypes of dry eye disease: a pilot in vivo confocal microscopic study. Invest Ophthalmol Vis Sci. 2015; 56:7179–85. [PubMed: 26540656]
39. Meijering E, Jacob M, Sarria JC, Steiner P, Hirling H, Unser M. Design and validation of a tool for neurite tracing and analysis in fluorescence microscopy images. Cytometry Part A: the journal of the International Society for Analytical Cytology. 2004; 58:167–76. [PubMed: 15057970]
40. Patel DV, McGhee CN. Laser scanning in vivo confocal microscopy demonstrating significant alteration of human corneal nerves following herpes zoster ophthalmicus. Arch Neurol. 2010; 67:640–1. [PubMed: 20457969]
41. Mayer WJ, Irschick UM, Moser P, Wurm M, Huemer HP, Romani N, et al. Characterization of antigen-presenting cells in fresh and cultured human corneas using novel dendritic cell markers. Invest Ophthalmol Vis Sci. 2007; 48:4459–67. [PubMed: 17898266]
42. Hamrah P, Zhang Q, Liu Y, Dana MR. Novel characterization of MHC class IInegative population of resident corneal Langerhans cell-type dendritic cells. Invest Ophthalmol Vis Sci. 2002; 43:639–46. [PubMed: 11867578]
43. Dana MR, Hamrah P. Role of immunity and inflammation in corneal and ocular surface disease associated with dry eye. Adv Exp Med Biol. 2002; 506:729–38.
44. Hamrah P, Chen L, Zhang Q, Dana MR. Novel expression of vascular endothelial growth factor receptor (VEGFR)-3 and VEGF-C on corneal dendritic cells. Am J Pathol. 2003; 163:57–68. [PubMed: 12819011]
45. Hamrah P, Huq SO, Liu Y, Zhang Q, Dana MR. Corneal immunity is mediated by heterogeneous population of antigen-presenting cells. J Leukoc Biol. 2003; 74:172–8. [PubMed: 12885933]
46. Hamrah P, Liu Y, Zhang Q, Dana MR. Alterations in corneal stromal dendritic cell phenotype and distribution in inflammation. Arch Ophthalmol. 2003; 121:1132–40. [PubMed: 12912691]
47. Zhivov A, Stave J, Vollmar B, Guthoff R. In vivo confocal microscopic evaluation of Langerhans cell density and distribution in the normal human corneal epithelium. Graefes Arch klin exp Ophthalmol. 2005; 243:1056–61.
48. Lin H, Li W, Dong N, Chen W, Liu J, Chen L, et al. Changes in corneal epithelial layer inflammatory cells in aqueous tear-deficient dry eye. Invest Ophthalmol Vis Sci. 2010; 51:122–8. [PubMed: 19628746]
49. Cruzat A, Schrems WA, Schrems-Hoesl LM, Cavalcanti BM, Baniasadi N, Witkin D, et al. Contralateral clinically unaffected eyes of patients with unilateral infectious keratitis demonstrate a sympathetic immune response. Invest Ophthalmol Vis Sci. 2015; 56:6612–20. [PubMed: 26465889]
50. Yamaguchi T, Calvacanti BM, Cruzat A, Qazi Y, Ishikawa S, Osuka A, et al. Correlation between human tear cytokine levels and cellular corneal changes in patients with bacterial keratitis by in vivo confocal microscopy. Invest Ophthalmol Vis Sci. 2014; 55:7457–66. [PubMed: 25324281]
51. Hamrah P, Seyed-Razavi Y, Yamaguchi T. Translational immunoimaging and neuroimaging demonstrate corneal neuroimmune crosstalk. Cornea. 2016; 35(Suppl 1):S20–S4. [PubMed: 27631352]
52. Sirinek LP, O'Dorisio MS. Modulation of immune function by intestinal neuropeptides. Acta Oncol. 1991; 30:509–17. [PubMed: 1713037]
53. McGillis JP, Mitsuhashi M, Payan DG. Immunomodulation by tachykinin neuropeptides. Ann N Y Acad Sci. 1990; 594:85–94. [PubMed: 1696081]
54. Schauenstein K, Rinner I, Felsner P, Mangge H. Bidirectional interaction between immune and neuroendocrine systems. An experimental approach. Padiatr Padol. 1992; 27:81–5. [PubMed: 1328993]
55. Sternberg EM. Neural regulation of innate immunity: a coordinated nonspecific host response to pathogens. Nat Rev Immunol. 2006; 6:318–28. [PubMed: 16557263]

56. Namavari A, Chaudhary S, Ozturk O, Chang JH, Yco L, Sonawane S, et al. Semaphorin 7a links nerve regeneration and inflammation in the cornea. Invest Ophthalmol Vis Sci. 2012; 53:4575–85. [PubMed: 22700709]
57. Brennan NA, Bruce AS. Esthesiometry as an indicator of corneal health. Optom Vis Sci. 1991; 68:699–702. [PubMed: 1745494]
58. Oliveira-Soto L, Efron N. Morphology of corneal nerves using confocal microscopy. Cornea. 2001; 20:374–84. [PubMed: 11333324]
59. Cruzat A, Qazi Y, Hamrah P. In vivo confocal microscopy of corneal nerves in health and disease. The Ocul Surf. 2017; 15:15–47. [PubMed: 27771327]
60. Oaklander AL. The density of remaining nerve endings in human skin with and without postherpetic neuralgia after shingles. Pain. 2001; 92:139–45. [PubMed: 11323135]
61. Millodot M. A review of research on the sensitivity of the cornea. Ophthalmic Physiol Opt. 1984; 4:305–18. [PubMed: 6390296]
62. Scholz J, Woolf CJ. The neuropathic pain triad: neurons, immune cells and glia. Nat Neurosci. 2007; 10:1361–8. [PubMed: 17965656]
63. Wolf G, Gabay E, Tal M, Yirmiya R, Shavit Y. Genetic impairment of interleukin-1 signaling attenuates neuropathic pain, autotomy, and spontaneous ectopic neuronal activity, following nerve injury in mice. Pain. 2006; 120:315–24. [PubMed: 16426759]
64. Arruda JL, Sweitzer S, Rutkowski MD, DeLeo JA. Intrathecal anti-IL-6 antibody and IgG attenuates peripheral nerve injury-induced mechanical allodynia in the rat: possible immune modulation in neuropathic pain. Brain Res. 2000; 879:216–25. [PubMed: 11011025]
65. Junger H, Sorkin LS. Nociceptive and inflammatory effects of subcutaneous TNFalpha. Pain. 2000; 85:145–51. [PubMed: 10692613]
66. Head H, Campbell AW, Kennedy PG. The pathology of Herpes Zoster and its bearing on sensory localisation. Rev Med Virol. 1997; 7:131–43. [PubMed: 10398478]
67. Oaklander AL, Romans K, Horasek S, Stocks A, Hauer P, Meyer RA. Unilateral postherpetic neuralgia is associated with bilateral sensory neuron damage. Ann Neurol. 1998; 44:789–95. [PubMed: 9818935]
68. Hamrah P, Sahin A, Oaklander AL. Widespread effects of clinically unilateral focal nerve injuries. Pain. 2017; 158:1175–6. [PubMed: 28514253]
69. Yamaguchi T, Turhan A, Harris DL, Hu K, Pruss H, von Andrian U, et al. Bilateral nerve alterations in a unilateral experimental neurotrophic keratopathy model: a lateral conjunctival approach for trigeminal axotomy. PLoS ONE. 2013; 8:e70908. [PubMed: 23967133]
70. Rokx JT, Juch PJ, Van Willigen JD. On the bilateral innervation of masticatory muscles: a study with retrograde tracers. J Anat. 1985; 140(Pt 2):237–43. [PubMed: 2416722]
71. Pfaller K, Arvidsson J. Central distribution of trigeminal and upper cervical primary afferents in the rat studied by anterograde transport of horseradish peroxidase conjugated to wheat germ agglutinin. J Comp Neurol. 1988; 268:91–108. [PubMed: 3346387]
72. Jacquin MF, Chiaia NL, Rhoades RW. Trigeminal projections to contralateral dorsal horn: central extent, peripheral origins, and plasticity. Somatosens Mot Res. 1990; 7:153–83. [PubMed: 2378191]
73. Clarke WB, Bowsher D. Terminal distribution of primary afferent trigeminal fibers in the rat. Exp Neurol. 1962; 6:372–83. [PubMed: 14021584]
74. Miyakoshi A, Takemoto M, Shiraki K, Hayashi A. Varicella-zoster virus keratitis with asymptomatic conjunctival viral shedding in the contralateral eye. Case Rep Ophthalmol. 2012; 3:343–8. [PubMed: 23162462]
75. Streilein JW, Dana MR, Ksander BR. Immunity causing blindness: five different paths to herpes stromal keratitis. Immunol Today. 1997; 18:443–9. [PubMed: 9293161]
76. Guthoff RF, Zhivov A, Stachs O. In vivo confocal microscopy, an inner vision of the cornea - a major review. Clin Exp Ophthalmol. 2009; 37:100–17. [PubMed: 19338608]
77. Knickelbein JE, Buela KA, Hendricks RL. Antigen-presenting cells are stratified within normal human corneas and are rapidly mobilized during ex vivo viral infection. Invest Ophthalmol Vis Sci. 2014; 55:1118–23. [PubMed: 24508792]

78. Murphy PJ, Lawrenson JG, Patel S, Marshall J. Reliability of the non-contact corneal aesthesiometer and its comparison with the Cochet-Bonnet aesthesiometer. Ophthalmic Physiol Opt. 1998; 18:532–9. [PubMed: 10070549]

79. Golebiowski B, Papas E, Stapleton F. Assessing the sensory function of the ocular surface: implications of use of a non-contact air jet aesthesiometer versus the Cochet- Bonnet aesthesiometer. Exp Eye Res. 2011; 92:408–13. [PubMed: 21376718]

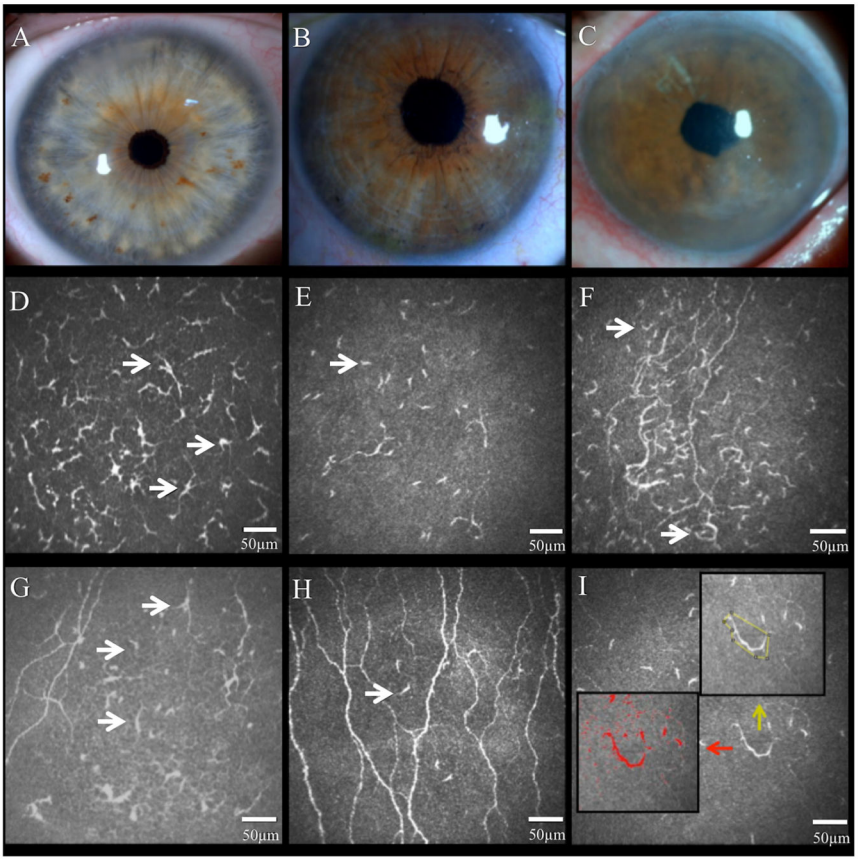


**Figure 1.**

Slit-lamp images of control eye (A), clinically unaffected contralateral eye (B), and affected eye with herpes zoster ophthalmicus (HZO) (C). Representative laser *in vivo* confocal microscopy images of corneal dendritiform immune cells (DCs) in the affected eye (D and E) and contralateral eyes of HZO patient (F and G), and normal control eye (H). Note the increase of DC density in both eyes of HZO patients. DC morphology analysis (I; in red DC size; yellow number of dendrites and DC field). Black arrows highlight DCs.

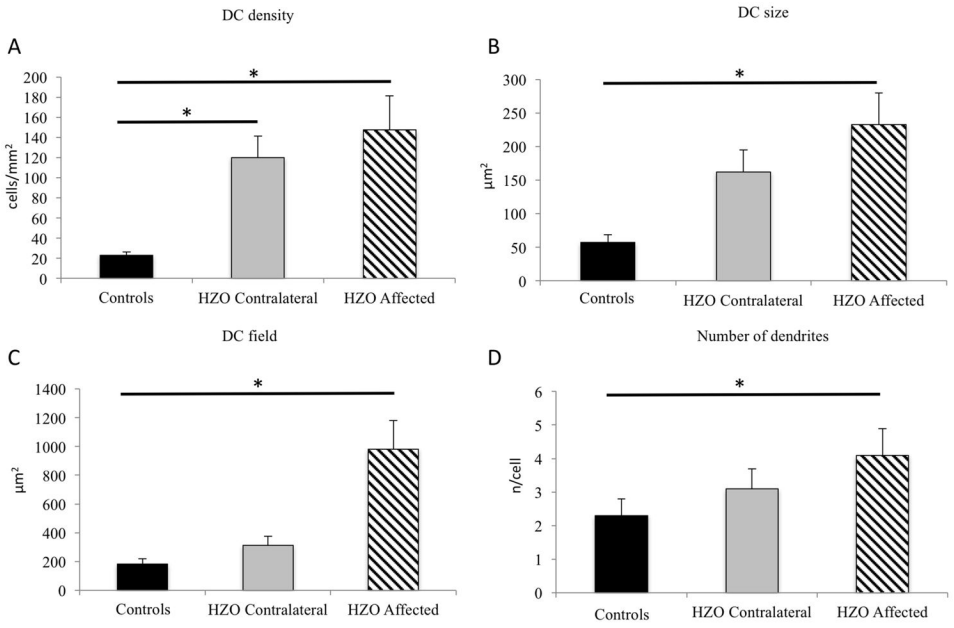


**Figure 2.**

Dendritiform immune cell density (DCs) in herpes zoster ophthalmicus. Affected and contralateral eyes reveal statistical significant increase of DC density (A). DCs in the affected eye showed an increase in size (B), as well as DC field (C) and in number of dendrites (D). (* statistical significant adjusted p-value< 0.05)

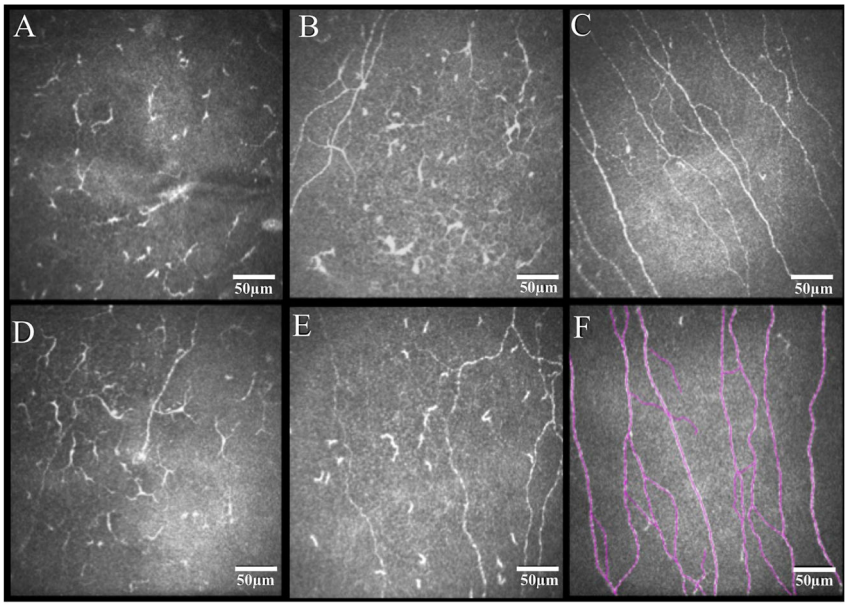


**Figure 3.**

Representative *in vivo* confocal microscopy images of the subbasal corneal nerve plexus in eyes with herpes zoster ophthalmicus and controls. Diminishment of nerve fibers is revealed in both affected eyes (A and D) and contralateral clinically unaffected eyes (B and E) of herpes zoster patients in comparison to normal controls (C). Example of nerve tracings performed by NeuronJ/ImageJ is shown (F).

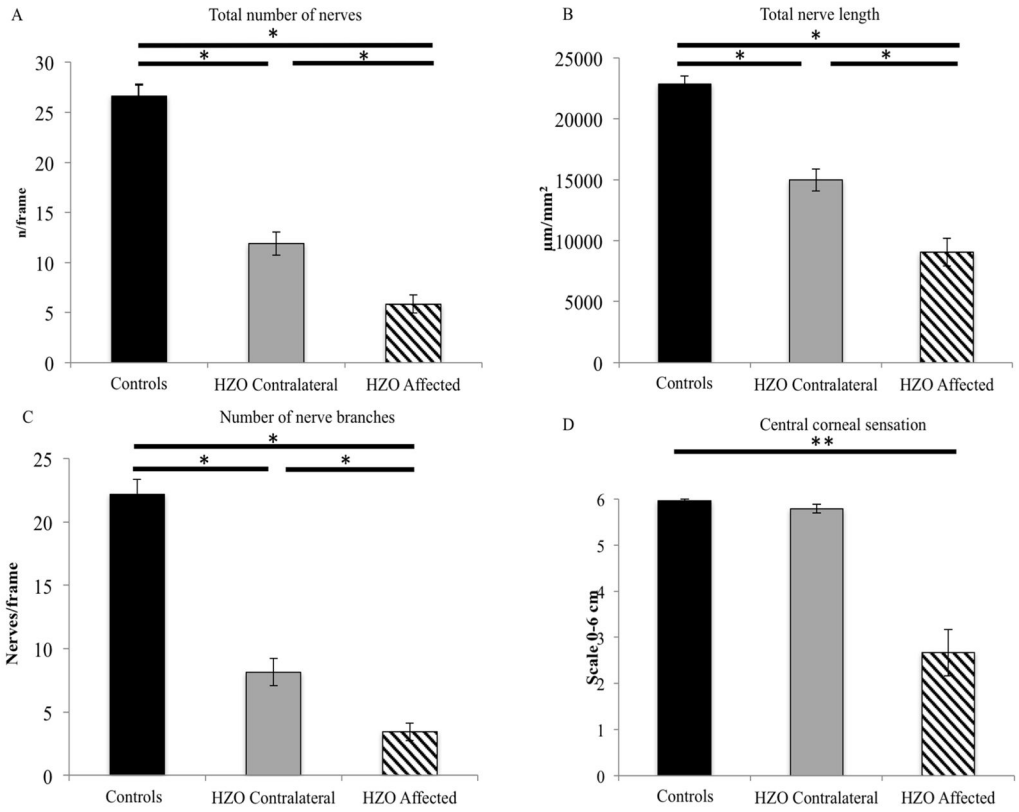


**Figure 4.**

Corneal nerves parameters in herpes zoster ophthalmicus. Both eyes of herpes zoster patients show a decrease of subbasal nerve parameters in comparison to controls. Number of total nerves (A) and total nerve length fibers (B), number of nerve branches (C), and central corneal sensation (D) for all groups. (*statistical significant adjusted p-value< 0.05).

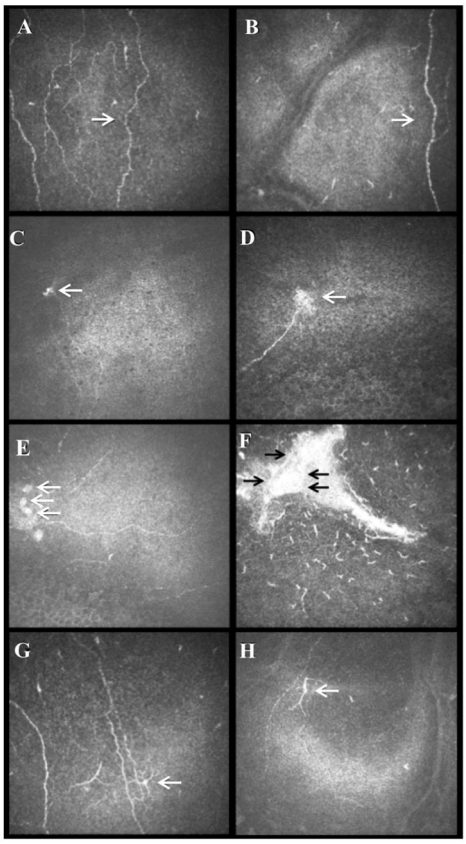


**Figure 5.**

Subbasal nerve features of in patients with pain from herpes zoster ophthalmicus. Representative *in vivo* confocal images of beading (A and B), neuromas (C and D), cluster of nuclei (E and F), and activated dendritic cells close to nerve fibers (G and H).

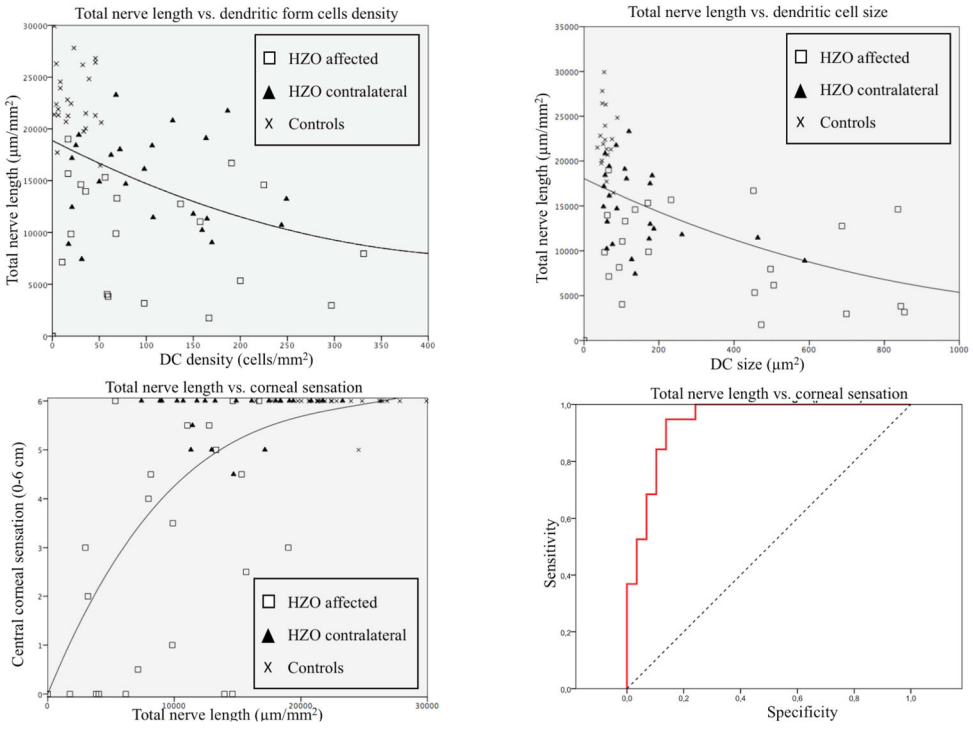


**Figure 6.**

Correlation for *in vivo* confocal microscopy parameters and corneal sensation. Total nerve length vs dendritic form cells density (A) and dendritic-form cells size (B) reveals positive correlation (R=−0.43 and R=−0.57, respectively). Total nerve length shows good positive correlation with corneal sensation (C)(R=0.63). ROC curve model demonstrates good specificity and sensitivity for detection of corneal sensation diminishment.

**Table 1**

Demographic data of normal controls and patients with herpes zoster ophthalmicus.

| | Controls | HZO | P value |
|---|---|---|---|
| Number of patients (n) | 24 | 24 | n/a |
| Age (years) | 55.6 ± 1.9 | 60.1 ± 3.0 | 0.2 |
| Gender (male/female) | 9/15 | 11/13 | 0.5 |
| Sensation (cm) | 5.9 ± 0.04 | 2.7 ± 0.5 | <0.0001 |
| Disease duration (months) | n/a | 57.0 ± 11.3 | n/a |
| Number of episodes (n) | n/a | 2.1 ± 0.3 | n/a |
| Time from last episode (months) | n/a | 30.4 ± 10.6 | n/a |
| Number of patients by location of scar (no scar/central/peripheral) | n/a | 5/11/8 | n/a |

Values are expressed as mean ± standard error of the mean.

HZO: Herpes zoster ophthalmicus; n/a: not applicable

**Table 2**

Dendritiform cell parameters and corneal subbasal nerve plexus parameters in control groups, contralateral unaffected eyes and affected eyes with herpes zoster ophthalmicus.

| | HZO affected | HZO contralateral | Controls |
|---|---|---|---|
| Eyes (n) | 24 | 24 | 24 |
| Mean central corneal sensation (cm) | 2.7 ± 0.5 * | 5.8 ± 0.1 | 5.9 ± 0.04 |
| DC density (cells/mm$^2$) | 147.4 ± 33.9 * | 120.1 ± 21.2 * | 23.0 ± 3.6 |
| DC size (μm$^2$) | 232.4 ± 47.4 * | 161.9 ± 33.1 | 57.2 ± 11.7 |
| DC field (μm$^2$) | 980.9 ± 200.2 * | 312.0 ± 63.7 * | 182.4 ± 37.2 |
| DC number of dendrites (n/cell) | 4.1 ± 0.8 * | 3.1 ± 0.6 | 2.3 ± 0.5 |
| Main nerve trunk length | 4,950.9 ± 662.9 * | 8,327.0 ± 474.9 * | 10,364.5 ± 355.6 |
| (μm/mm2)/[μm/frame] | [792.1 ± 106.1] | [1,332.3 ±76.0] | [1,658.3 ± 57.0] |
| Nerve branch length | 4,101.6 ± 538.7 * | 6,521.7 ± 681.0 * | 12,486.9 ± 522.1 |
| (μm/mm$^2$)/[μm/frame] | [656.3 ± 86.2] | [1,043.5 ± 109.0] | [1,997.9 ± 83.5] |
| Total nerve length | 9,052.6 ± 1151.4 * | 14,959.8 ± 903.2 * | 22,851.4 ± 661.4 |
| (μm/mm$^2$)/[μm/frame] | [1,448.4 ± 184.2] | [2,393.6 ± 144.5] | [3,656.2 ±105.8] |
| Number of main nerve trunks (n/frame) | 2.4 ± 0.3 * | 3.8 ± 0.3 | 4.4 ± 0.2 |
| Number of nerve branches (n/frame) | 3.4 ± 0.7 * | 8.2 ± 1.1 * | 22.2 ± 1.2 |
| Total number of nerves (n/frame) | 5.8 ± 0.9 * | 11.9 ± 1.2 * | 26.6 ± 1.2 |

Values are expressed as mean ± standard error of mean.

* Statistically significant ($p<0.05$) compared to controls.

HZO: Herpes Zoster Ophthalmicus, DC: Dendritiform cell.

**Table 3**

Dendritiform cell parameters and corneal subbasal nerve plexus parameters in affected eyes with or without pain in herpes zoster ophthalmicus.

| | Patients with pain | Patients without pain | P value |
|---|---|---|---|
| n | 14 | 10 | n/a |
| Age (years) | 60.1±16.4 | 60.0±12.5 | 0.9 |
| Sensation (cm) | 2.6±2.1 | 2.6±2.7 | 0.9 |
| DC density (cells/mm$^2$) | 136.3±59.2 | 143.7±42.4 | 0.9 |
| DC size (μm$^2$) | 225.5±87.3 | 366.2±77.5 | 0.2 |
| DC field (μm$^2$) | 615.3±341.3 | 874.1±184.0 | 0.4 |
| DC number of dendrites (n/cell) | 4.3±1.0 | 3.0±0.3 | 0.1 |
| Main nerve trunk length (μm/mm$^2$)/[μm/frame] | 4409.3±1091.1 [705.4±174.5] | 5221.8±847.5 [835.4±135.6] | 0.5 |
| Nerve branch length (μm/mm$^2$)/[μm/frame] | 3472.2±861.6 [555.5±137.8] | 4416.2±688.6 [706.5±110.1] | 0.4 |
| Total nerve length (μm/mm$^2$)/[μm/frame] | 7881.6±1926.9 [1261.0±308.3] | 9636.0±1454.7 [1541.7±232.7] | 0.4 |
| Number of main nerve trunks (n/frame) | 2.2±0.4 | 2.4±0.3 | 0.7 |
| Number of nerve branches (n/frame) | 2.2±0.4 | 4.0±0.9 | 0.2 |
| Total number of nerves (n/frame) | 4.4±1.1 | 6.5±1.1 | 0.2 |

Values are expressed as mean ± standard error of the mean. n/a: not applicable